

On the Upper Bound of the Information Capacity in Neuronal Synapses

Mladen Veletić, *Student Member, IEEE*, Pål Anders Floor, Youssef Chahibi, *Student Member, IEEE* and Ilangko Balasingham, *Senior Member, IEEE*

Abstract—Neuronal communication is a biological phenomenon of the central nervous system that influences the activity of all intra-body nano-networks. The implicit biocompatibility and dimensional similarity of neurons with miniature devices make their interaction a promising communication paradigm for nano-networks. To understand the information transfer in neuronal networks, there is a need to characterize the noise sources and unreliability associated with different components of the functional apposition between two cells – the synapse. In this paper, we introduce analogies between the optical communication system and neuronal communication system to apply results from optical Poisson channels in deriving theoretical upper bounds on the information capacity of both bipartite- and tripartite synapses. The latter refer to the anatomical and functional integration of two communicating neurons and surrounding glia cells. The efficacy of information transfer is analyzed under different synaptic set-ups with progressive complexity, and is shown to depend on the peak rate of the communicated spiking sequence and neurotransmitter (spontaneous) release, neurotransmitter propagation, and neurotransmitter binding. The results provided serve as a progressive step in the evaluation of the performance of neuronal nano-networks and the development of new artificial nano-networks.

Index Terms—Synaptic Transmission, Poisson Channel, Channel Capacity, Neuronal Nano-Network, Intra-Body Communications.

I. INTRODUCTION

THE beauty of Shannon’s information theory is the generality that encompasses all communication and processing systems regardless of whether the signals communicated are digital or analog. This enables researchers to deploy information theory to numerous fields, including the analysis of biological communication systems such as the brain and *neuronal communication networks*, where the signals involved are analog.

Neurons are analyzed and involved by the ICT community in the creation of artificial neural-like nano-networks for intra-body communications [1]–[5]. They respond with stochastic

M. Veletić is with the Department of Electronics and Telecommunications, Norwegian University of Science and Technology (NTNU), 7491 Trondheim, Norway, and with the Faculty of Electrical Engineering, University of Banja Luka (UNIBL), 78000 Banja Luka, Bosnia and Herzegovina.

P. A. Floor and I. Balasingham are with the Intervention Center, Oslo University Hospital and Institute of Clinical Medicine, University of Oslo, 0372 Oslo, Norway, and with the Department of Electronics and Telecommunications Norwegian University of Science and Technology (NTNU), 7491 Trondheim, Norway.

Y. Chahibi is with the Broadband Wireless Networking Laboratory, School of Electrical and Computer Engineering, Georgia Institute of Technology, Atlanta, GA 30332, USA.

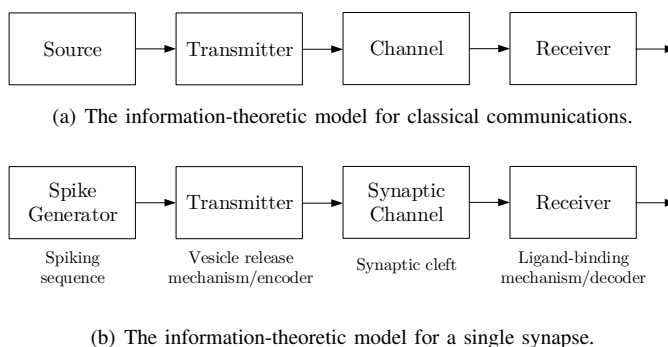


Fig. 1. The classical information theory model and its equivalent in the neuroscience. Figure adapted by authors from [7, Chapter 3].

action potentials (spiking sequences) that are further communicated over synapses which are often unreliable. Although it is not clear whether this unreliability is a ‘bug’ or a ‘feature’ of neurons [6], the question that arises is: How does one examine measurements to determine how close to the limits the neuronal system is operating [7]? Here comes another beauty of information theory and the ability to transform the previous question to: How effectively does the output represent the input? Henceforth, instead of finding good measurement techniques in assessing effectiveness and establishing performance limits, the key information-theoretic quantities are used [8]. Fig. 1(a) shows the well-established model underlying classical information theory [7], [8].

The available information-theoretic analysis are ubiquitously applied to a *single neuron* to obtain theoretic quantities on how much information a neuronal output/response carries about the time-varying input/stimulus (see [7], [9]–[13], and references therein). Unlike these analysis, we apply information theory to a *single synapse* with an objective to quantify how much information a receiving/post-synaptic neuron carries about the transmitting/pre-synaptic neuron. The synaptic channel capacity is investigated with particular emphasis since the communication paradigms within a synapse and within a single neuron are phenomenologically different. Namely, the communication within a synapse in a neuron-to-neuron communication channel means the **molecular transmission** of particles (neurotransmitters) from the pre-synaptic terminal to the post-synaptic terminal. The communication within a neuron, however, means the **electrochemical transmission** of ions, e.g., Na^+ , Ca^{2+} , K^+ and Cl^- [14]. The information-theoretic model for a single synapse is shown in Fig. 1(b).

Let us get back to the quantification on how much infor-

mation the spiking sequence carries about the stimulus where two methods are straightforward [10]. The first is the ‘direct’ method of calculating mutual information from the neuronal response R by estimating its entropy, $H(R)$, and neuronal noise, $H(R|S)$, i.e.,

$$I(R, S) = H(R) - H(R|S). \quad (1)$$

In this method, the spike train noise is determined by repeating a dynamic stimulus many times to get the response distribution under the same stimulus conditions. The second method adds the assumption that the neuronal response amplitudes have Gaussian probability distributions in the frequency domain, and computes an upper bound on mutual information – *capacity*. These approaches, however, can be adopted to the analysis of noisy and unreliable synapses. As an example, if the capacity is estimated, one should assume i) the post-synaptic response¹ amplitudes have Gaussian probability distribution in the frequency domain [15], ii) the stimulus S is the mean post-synaptic response obtained from many repetitions of identical stimulus conditions, and iii) the actual response R is the response on individual trials, which equals the mean signal plus a noise term. With this approach, one does not need knowledge on neuronal physiology and information processing. It is enough to treat a channel as a black box and apply tools from statistical estimation theory in estimating the capacity from empirically recorded input and output signals. This is unambiguously the advantage of this approach. The disadvantage is, however, that one must collect data to estimate theoretical limits. But, can we understand neuronal compartments (peculiarly those forming the synapse) as communication devices and bypass the need to record the data?

¹The post-synaptic response can be referred to as changes in the membrane potential of the post-synaptic terminal that should not be confused with action potentials, or to the current that causes changes in membrane potential.

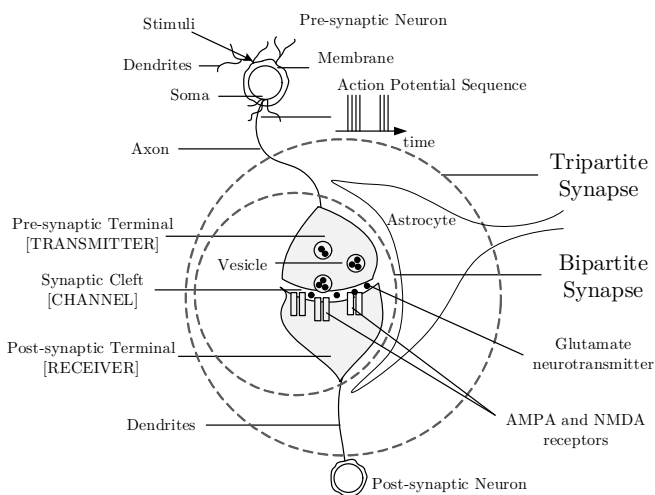


Fig. 2. Schematic diagram of the neuronal anatomy with bipartite and tripartite synapses. Alike neurons, astrocytes can release glutamate into the cleft in response to an increased activity of adjacent neurons, acting as feedback units to the neuron.

The knowledge about the neuronal anatomy, physiology, and the manner in which information is processed and communicated at various stages in single neurons has accumulated [6], [7], [16]. The main neuronal compartments with two possible configurations forming the concepts of bipartite and tripartite synapses are depicted in Fig. 2. The *bipartite synapse* is an important component of the communication channel between neurons. Specifically, it is the site of functional apposition between two cells, where a transmitting pre-synaptic neuron/terminal converts the spiking signal into neurotransmitter molecules, that are released into the synaptic cleft to propagate and bind to the AMPA (α -amino-3-hydroxy-5-methyl-4-isoxazolepropionic acid) and NMDA (N-methyl-D-aspartate) receptors² located on the membrane of the receiving post-synaptic neuron/terminal. When the astrocyte cell is in the vicinity of the synapse, the concept of *tripartite synapse* is introduced to underline the presence of the astrocytic terminal in the vicinity of two neurons. An astrocyte is a particular star-shaped type of neuroglia which fills the spaces between neurons. Astrocytes cannot produce spikes and therefore were not initially suspected as playing an important and active role in neuronal communication. However, they are numerous, accounting for over 70% of all cells in the central nervous system (this number is specific for higher mammals), and are now known to appreciably support neuronal functions and intercellular coordination. The mechanisms behind tripartite synapse and feedback provided from astrocytes are complex and take into account several physiological processes. The reader is referred to [17]–[20] for details.

Concerning the synaptic communication channel, the closest related work is the work by Manwani and Koch [21] who relied on neuronal hardware to look at the issue of information transmission over unreliable synapses. They derived *theoretical lower bounds on the information capacity* of a simple model of the bipartite synapse under signal estimation and signal detection paradigms. The first assumes the information to be encoded in the mean spiking rate/intensity of the pre-synaptic neuron, with the objective to estimate the continuous input signal from the post-synaptic response. The second observes the input as binary, and the presence or absence of a pre-synaptic spike is to be detected from the post-synaptic response.

As spoken of earlier, the ultimate goal of this paper is to quantify how much information a receiving/post-synaptic neuron carries about the transmitting/pre-synaptic neuron. This quantification should provide a supplementary insight into the efficacy of information transmission between neurons by deriving *theoretical upper bounds on the information capacity* of bipartite and tripartite synapses. To this end, we tackle different system models and set-ups (relative to [21]) with progressive complexity and analyze a noisy bipartite synapse with: i) reliable vesicle³ release, ii) unreliable vesicle release

²In case the neuroplasticity (dynamic wiring of neurons) is not considered (as in this study), it is common in neuroscience to analyze only AMPA receptors since they mediate most of the synaptic excitation in the central nervous system. Otherwise, NMDA receptors are also important.

³A vesicle is a small structure within a cell containing neurotransmitters (see Fig. 2).

with constant release probability, iii) unreliable vesicle release with time-varying release probability, and iv) unreliable vesicle release followed by an unreliable neurotransmitter propagation and binding to the receiving neuron. Then, we extend analysis to the concept of a noisy and unreliable tripartite synapse. The findings and results shall be of primary importance in understanding the performance of the neuronal communication paradigm as a candidate for future nano-networks.

The remainder of this paper is organized as follows. Section II defines a system model used for capacity computation. Section III provides a brief introduction to the recognized analogies between neuronal and optical communication systems vastly used throughout the paper. The theoretical upper bounds on the capacity of a synapse under the five scenarios defined above are derived in Section IV, and plotted in Section V. An illustrative example of a realistic hippocampal channel is considered in Section VI. Our concluding remarks and notes on future work are given in Section VII.

II. SYSTEM MODEL

Given the stimuli $\theta(t)$ at the input of the pre-synaptic neuron (refer to Fig. 2), which is typically a dendritic current, I_d , or somatic current, I_s , the spike encoder generates a sequence of action potentials encoding the information contained in the stimulus. The simplest model of the spike train is the non-homogeneous Poisson process [22] with rate depending on the magnitude of the stimulus. However, the neuronal membrane is refractory immediately after a spike, which leads to the firing probability that depends not only on the stimulus but also on the preceding spike train. As a consequence, the refractoriness precludes two consecutive spikes to be independent and causes the spike train to become more regular than a Poisson process with the same firing rate [13]. Thus, a more theoretically grounded way would be to modify the Poisson process to include refractoriness. Albeit Berry and Meister [23] did that way by defining the instantaneous firing rate as the product of a *free firing rate*, which depends only on the stimulus, and a *recovery function*, which depends only on the time since the last spike, they proved the free firing to be a more fundamental response measure if neurons use a “firing rate code” in which the message lies in the instantaneous spiking. A refractory period actually causes the modified rate to saturate and miss out gradations in the stimulus. Motivated by this inference, we practically neglect the refractoriness in the synaptic capacity analysis; we believe that a spiking sequence $v(t)$ described as a *non-homogeneous Poisson impulse process* directed by the intensity that is proportional to the stimulus, i.e., $\lambda_1(t) \propto \theta(t)$, is adequate for derivation of upper bounds on information rates in neuronal synapses. Thus,

$$v(t) = \sum_{n=1}^{N_1(t)} \delta(t - t_n), \quad (2)$$

where t_n is the arbitrary spike generation time, and $\{N_1(t) : 0 \leq t \leq T\}$ is a non-homogeneous Poisson process whose rate, $\lambda_1(t)$, is a temporal function, and

$$\mathbb{E}[N_1(t)] = \int_0^t \lambda_1(u) du. \quad (3)$$

The operator $\mathbb{E}[\cdot]$ denotes expectation. The signal $v(t)$ propagates down the axon, a nerve fiber that conducts impulses away from the neuron’s body (see Fig. 2), and reaches the pre-synaptic terminal of the transmitting neuron.

Numerous physiological mechanisms [14], [17], [24] convert the spiking sequence $v(t)$ into a chemical form $q(t)$ generated by means of neurotransmitter release machinery.

- The release of neurotransmitters upon arrival of individual action potentials is modulated by the **vesicle release probability**, P_{rel} , driven by the intracellular calcium concentration within the pre-synaptic terminal of the transmitting neuron, $[Ca^{2+}]_{pre}$. For the tripartite synapse, $[Ca^{2+}]_{pre}$ is found from the Pinsky-Li-Rinzel model [19], [20], [25], [26]. The relation between $[Ca^{2+}]_{pre}$ and P_{rel} is found from the Bertram-Sherman-Stanley four-gate model of the vesicle release process. The model contains four independent gates ($S_1 - S_4$) with different opening and closing rates, and with S_4 closing most rapidly and S_1 closing most slowly, i.e., [27]

$$P_{rel}(t) = O_1(t)O_2(t)O_3(t)O_4(t), \quad (4)$$

where O_j s are the open gate probabilities associated with gates S_j s, and

$$\frac{dO_j(t)}{dt} = k_j^+[Ca^{2+}]_{pre}(t) - \frac{O_j(t)}{\tau_j}, \quad j = 1, 2, 3, 4. \quad (5)$$

k_j^+ and k_j^- are opening and closing rates ($ms^{-1} \times \mu M^{-1}$), respectively: $k_1^+ = 3.75 \times 10^{-3}$, $k_1^- = 4 \times 10^{-4}$, $k_2^+ = 2.5 \times 10^{-3}$, $k_2^- = 1 \times 10^{-3}$, $k_3^+ = 5 \times 10^{-4}$, $k_3^- = 0.1$, $k_4^+ = 7.5 \times 10^{-3}$, $k_4^- = 10$, and $\tau_j = 1/(k_j^+[Ca^{2+}]_{pre} + k_j^-)$.

Owing to the property of splitting non-homogeneous Poisson processes [28], we define the neurotransmitter sequence that is injected into the synaptic cleft by the pre-synaptic terminal as a non-homogeneous Poisson process given as

$$q(t) = \sum_{n=1}^{N_2(t)} q_n \delta(t - t_n), \quad (6)$$

where q_n is the number of injected neurotransmitters at the arbitrary time t_n , $\{N_2(t) : 0 \leq t \leq T\}$ is a non-homogeneous Poisson process, and

$$\mathbb{E}[N_2(t)] = \int_0^t P_{rel}(u) \lambda_1(u) du. \quad (7)$$

There are two more sources of unreliability in the remaining communication pathway between two neurons:

- The neurotransmitter propagation towards the post-synaptic membrane is random and caused by the stochastic nature of the Brownian motion of neurotransmitters in a fluid medium of synaptic cleft. Based on the analogy between the advection-diffusion equation and the Fokker-Planck equation, Chahibi and Akyildiz [28] found a single drug particle delivery in particulate drug delivery system within the cardiovascular network to follow a Bernoulli distribution. The advection-diffusion equation is based on the generalized Taylor dispersion equation that governs

the crosssectional concentration of particles. The Fokker-Planck equation is the basis of the random motion of particles. As the mentioned analogy is valid in fluid synaptic cleft, a single neurotransmitter delivery (*not* binding), described with the **neurotransmitter propagation probability**, P_s , should then also follow a Bernoulli distribution.

- The neurotransmitter binding to the membrane of the post-synaptic neuron is characterized by the ligand-binding mechanism. The first time derivative of the probability of having n_b bound receptors among the N_R receptors, dP_{n_b}/dt , is found to depend on three terms: the probability P_{n_b-1} of having $n_b - 1$ bound chemical receptors and having a binding reaction, the probability P_{n_b+1} of having $n_b + 1$ bound chemical receptors and having a release reaction, and the negative of the probability P_{n_b} of having either a release reaction or a binding reaction [29], i.e.,

$$\begin{aligned} \frac{dP_{n_b}(t)}{dt} &= c_R(t)k_+(N_R - n_b + 1)P_{n_b-1}(t) \\ &+ k_-(n_b + 1)P_{n_b+1}(t) \\ &- [k_-n_b + c_R(t)k_+(N_R - n_b)]P_{n_b}(t). \end{aligned} \quad (8)$$

In (8), $c_R(t)$ is the neurotransmitter concentration, and k_+ and k_- are the neurotransmitter binding and release rates, respectively.

The binding of neurotransmitters to the AMPA and NMDA described with the **neurotransmitter binding probability**, P_b , similarly depends on the number of receptors in an open state. Hence, we define the first derivative of the probability P_b as

$$\frac{dP_b(t)}{dt} = c_R(t)k_+(N_R - n_b)P_b(t). \quad (9)$$

In a simplified scenario, the neurotransmitter binding probability, P_b , can be modeled to follow a Bernoulli distribution.

III. SYNAPTIC POISSON CHANNEL

Given the system model in previous section, we motivate with a principal analogy between the **optical communication system** and **synaptic communication system**. This principal analogy turns out to be essential to this study, as it enables the calculation of the capacity of a *Poisson-type synaptic channel*, using results derived for the optical communication channel. The capacity of the optical communication channel was found in [30]–[35].

The transmitter in the optical communication system is a *laser* and is related to the *pre-synaptic terminal* in the synaptic communication system. The channel in the optical communication system is an *optical fiber* and is related to the *synaptic cleft* in the synaptic communication system. The receiver in the optical communication system is a *photo-detector* and is related to the *post-synaptic terminal* in the synaptic communication system. The analogy stems from the following:

- At the transmitter in the optical communication system, a laser emits a stream of photons with a time-varying rate

that is proportional to the amplitude of the input current. It has been shown [36] that the emission of photons corresponds to the point process, and the transmitted beam fluctuations generated by a single-mode laser obey Poisson statistics. Hereof, the sequence of photons is typically modeled as a non-homogeneous Poisson point process with a time-varying rate [36], [37].

The analogy between the emissions of photons and neurotransmitters arises as the neurotransmitter sequence injected into the synaptic cleft by the pre-synaptic terminal can also be modeled as a non-homogeneous Poisson point process (see (6)) [22], as justified in the previous section.

- The relation between channels is of less relevance, but evident: the photon particles propagate through the fiber in the optical communication system; the neurotransmitter particles propagate/diffuse through the cleft in the synaptic communication system.
- A stream of photons is received by a photo-detector which is able to determine and count the arrival times of individual photons. The expectation of the count varies as the input signal that modulates the laser beam, plus the effect of noise [36]. The noise is due to detector “dark current” and background radiation, which is thought to obey Poisson statistics.

The analogy between the receptions of photons and neurotransmitters arises from the following. A stream of neurotransmitters is received by AMPA and NMDA receptors at the post-synaptic terminal. AMPA and NMDA receptors become conductive for Na^+ and K^+ ions leading to a change (increase) in post-synaptic membrane potential known as an Excitatory Post-Synaptic Potential (EPSP). Multiple EPSPs that are generated by the dendritic compartments of the receiving neuron sum up constructing a membrane potential that may lead to another spiking sequence⁴. As the photon counting process, the neurotransmitter binding and influx of ions into the receiving neuron varies as the input spiking sequence at the pre-synaptic terminal, plus the effect of noise. The noise here is due to spontaneous vesicle release, which is also thought to obey Poisson statistics [20].

Applying Poissonian spiking statistics and channel results in the capacity analysis of neurons has been done to quantify how much information a neuronal response carries about the time-varying stimulus [7, Chapter 3], [12], [13]. Although the Poissonian nature of the synaptic channels has been indicated every time the spiking sequence obeyed Poisson statistics, to the best of our knowledge this is the first time the analogies between the neuronal system and optical system are introduced. Apparently, applying the optical Poisson channel results to the capacity analysis of a neuronal synapse is done for the first time in the literature.

IV. THE SYNAPTIC CHANNEL CAPACITY

The synaptic Poisson channel is an additive noise channel with output $Y = N + X$, where N is the channel noise and

⁴With just one synapse and/or one incoming spiking sequence, the receiving neuron is not capable of generating another spiking sequence.

X is the transmitted signal into which the message $\theta(t)$ is encoded. Both N and X are Poisson-type point processes. N represents the **noisy effect** of spontaneous vesicle release and is directed by the intensity $\lambda'_0(t) = P_s(t)P_b(t)\lambda_0(t)$, where $\lambda_0(t)$ is the intensity of spontaneous release at the pre-synaptic terminal. X is directed by the spiking-dependent intensity $\lambda'_1(t, \lambda_1(t, \theta)) = P_{rel}(t)P_s(t)P_b(t)\lambda_1(t)$. Thus, the output Y is also a Poisson-type point process directed by the intensity

$$\begin{aligned}\lambda_2(t) &= \lambda'_0(t) + \lambda'_1(t, \lambda_1) \\ &= P_s(t)P_b(t) [\lambda_0(t) + P_{rel}(t)\lambda_1(t)].\end{aligned}\quad (10)$$

Note that λ'_0 and λ'_1 stem from the property of splitting non-homogeneous Poisson processes [28], and are valid only when the neurotransmitter release, propagation and binding processes are independent. We thoroughly consider this issue in Section IV-D.

The rate of the spontaneous vesicle releases, $\lambda_0(t)$, that can occur when the pre-synaptic membrane is not depolarized, depends on the pre-synaptic calcium concentration $[\text{Ca}^{2+}]_{pre}$ as [20]

$$\lambda_0(t) = a_3 \left(1 + e^{(a_1 - [\text{Ca}^{2+}]_{pre}(t))/a_2}\right)^{-1}.\quad (11)$$

The coefficients a_1 , a_2 and a_3 depend on the number of active zones, which are the sites of neurotransmitter release.

Given $\lambda_1(t) = \lambda_1$, the pre-synaptic calcium concentration is nontime-varying at the time instants of action potential arrivals, $[\text{Ca}^{2+}]_{pre}(t) = [\text{Ca}^{2+}]_{pre}$. In other words, the envelope of the concentration is nontime-varying, as we demonstrate later in Section VI. This assumption implies from (11) that $\lambda_0(t) = \lambda_0$ at the time instants of action potential arrivals. This is applicable to the bipartite synapse where the primal contribution to the calcium concentration is due to the action potentials arriving at the pre-synaptic terminal, i.e., $[\text{Ca}^{2+}]_{pre} = [\text{Ca}^{2+}]_{AP}$. For the tripartite synapse, the spontaneous vesicle release $\lambda_0(t)$ is time-varying, owing to additional contribution to the calcium concentration due to the astrocytic feedback (refer to [17]), i.e., $[\text{Ca}^{2+}]_{pre} = [\text{Ca}^{2+}]_{AP} + [\text{Ca}^{2+}]_{astro}$ (which produces the time-varying calcium concentration).

As mentioned earlier, we elaborate on the problem considering synapses with increasing complexity. For the sake of clarity, we are not going to consider at first the uncertainties induced by the particle propagation through the synaptic cleft and the ligand-binding mechanism, i.e., $P_s(t)$ and $P_b(t)$ are both unity. Under this simplification, the system models for the bipartite- and tripartite synapses are

$$\lambda_2(t) = \lambda_0 + P_{rel}(t)\lambda_1,\quad (12)$$

$$\lambda_2(t) = \lambda_0(t) + \tilde{P}_{rel}(t)\lambda_1,\quad (13)$$

respectively. Relative to $P_{rel}(t)$ in (12), $\tilde{P}_{rel}(t)$ in (13) is additionally affected by the astrocyte.

Throughout the paper, we analyze the information processing limits subject to the **rate amplitude constraint**

$$\lambda_2 \in [\lambda_0, \lambda_0 + \Lambda],\quad (14)$$

where Λ is the maximum spiking rate at the input, and an **average energy constraint**

$$\mathbb{E} \left[\int_0^T \lambda_2(t) dt \right] \leq (\Lambda_0 + \lambda_0)T,\quad (15)$$

where Λ_0 is an arbitrary spiking rate, $0 \leq \Lambda_0 \leq \Lambda$. The peak constraint given in (14) is associated with neuron's inability to fire with the rate higher than that physiologically determined as the neuronal membrane has an upper rate at which it can depolarize [16]. The maximum spiking rate varies among neuron types; refer to [38] for electrophysiological values of maximum firing rates across neuron types. The average energy constraint in (15) is directly associated with metabolically expensive neuron's signaling, as analysis of synaptic signaling confirmed that the nervous system use much energy to generate and communicate signals [39]. The resting metabolic energy thus naturally constraints the flow of information between synapses and limits neuronal performance and neuronal consumption.

A. Noisy and Reliable Vesicle Release

At the outset, let us begin with a special and simple case: the bipartite synapse with a vesicle release that is noisy – spontaneous vesicle releases occur without neuronal spiking, but reliable – vesicle releases follow the arrival of individual spikes to the pre-synaptic terminal. Hence, the vesicle release probability $P_{rel} \rightarrow 1$, and from (12) the output of the channel is a non-homogeneous Poisson process directed by the intensity $\lambda_2(t) \rightarrow \lambda_0 + \lambda_1(t)$. This means the channel output is only a noisy version of the channel input.

The optical counterpart of this problem is known in the literature; see the work by M. Davis [31]. At this point, we refer to fundamental analogies provided in Section III, and associate the upper bound for the synaptic Poisson channel capacity with the upper bound for the optical Poisson channel capacity. The analogy allows us to omit detailed derivation. When adapted to the synaptic Poisson channel, the upper bound is given as [35]

$$\mathcal{C}_{UB}^{(a)} = \max_{0 \leq \mu \leq \sigma} [\mu\phi(\Lambda) - \phi(\mu\Lambda)],\quad (16)$$

where $\phi(x) = (\lambda_0 + x) \ln(\lambda_0 + x) - \lambda_0 \ln \lambda_0$, μ is the probability of the channel input taking the value Λ , and σ is the ratio of average-to-peak power, $0 \leq \sigma \leq 1$. Eq. (16) is maximized for

$$\mu_{\max}^{(a)} = \frac{\lambda_0}{\Lambda} \left[\frac{1}{e} \left(1 + \frac{\Lambda}{\lambda_0}\right)^{(1+\lambda_0/\Lambda)} - 1 \right],\quad (17)$$

whence the *upper bound on the capacity for the bipartite synaptic Poisson channel with reliable vesicle release* is calculated as [31]

$$\mathcal{C}_{UB}^{(a)} = \begin{cases} \mu\phi(\Lambda) - \phi(\mu\Lambda), & \mu < \mu_{\max}^{(a)}, \\ \frac{\lambda_0}{e} \left(1 + \frac{\Lambda}{\lambda_0}\right)^{(1+\lambda_0/\Lambda)} - \lambda_0 \ln \left[\left(1 + \frac{\Lambda}{\lambda_0}\right)^{(1+\lambda_0/\Lambda)} \right], & \mu \geq \mu_{\max}^{(a)}. \end{cases}\quad (18)$$

$$\mathcal{C}_{UB}^{(b)} = \begin{cases} \mu\phi(p_{rel}\Lambda) - \phi(\mu p_{rel}\Lambda), & \mu < \mu_{max}^{(b)}, \\ \frac{\lambda_0}{e} \left(1 + \frac{p_{rel}\Lambda}{\lambda_0}\right)^{(1+(p_{rel}\Lambda)^{-1}\lambda_0)} - \lambda_0 \ln \left[\left(1 + \frac{p_{rel}\Lambda}{\lambda_0}\right)^{(1+(p_{rel}\Lambda)^{-1}\lambda_0)} \right], & \mu \geq \mu_{max}^{(b)}, \end{cases} \quad (24)$$

This result resembles the capacity of a single neuron cell described with a Poisson channel [7, Chapter 3], where the noise effects come from spontaneous spike generation. In case randomness in the synapse is involved, the data processing inequality [8] suggests the channel capacity must be less than or equal to (18).

B. Noisy and Unreliable Vesicle Release with Constant Release Probability

If the synaptic channel output is directed by the intensity

$$\lambda_2(t) = \lambda_0 + P_{rel}(t)\lambda_1(t), \quad (19)$$

where $P_{rel}(t) \in [0, 1]$, we can adapt the approach taken by Chakraborty and Narayan in the analysis of the optical Poisson fading channel [35], where the output rate is

$$\lambda_2(t) = \lambda_0 + S(t)\lambda_1(t), \quad (20)$$

with $S(t)$ representing the channel fade, and λ_0 the effect of “dark current” and background radiation in optical communication channel. The probability $P_{rel}(t)$ in (19) corresponds to the channel fade $S(t)$ in (20).

In this subsection, we derive the channel capacity for a noisy and unreliable bipartite synapse where vesicle releases follow the arrival of individual spikes to the pre-synaptic terminal with constant release probability. This problem can be associated with the scenario in optical communication system when channel fade in (20) is constant, i.e., $S(t) = s$, and the receiver possess perfect channel state information (CSI) while the transmitter has no CSI. The assumption of known CSI is pivotal for the mathematical tractability. Note that the best solution to this problem would be to derive the upper bound on information rate when neither the pre- and post-synaptic terminal would have the CSI. However, the unknown close-form bound without CSI at present is of primary importance in future research efforts since this will help in finding more exact capacity bounds for neuronal synapses. Furthermore, we prefer the case with known CSI at the post-synaptic side and no CSI at the pre-synaptic side over the case with perfect CSI at both the pre- and post-synaptic terminals, as the former is likely to be the tightest upper bound. Under these assumptions, the corresponding channel capacity is found as [35]

$$\mathcal{C} = \max_{0 \leq \mu \leq \sigma} [\mu\phi(s\Lambda) - \phi(\mu s\Lambda)], \quad (21)$$

where μ is the probability of the channel input taking the value Λ , σ is the ratio of average-to-peak power, $0 \leq \sigma \leq 1$, and s is the channel fade.

Unlike the problem of capacity calculation for Poisson channels [30], [31], capacity calculation for Poisson fading channels has to account for the output rate that is not only a noisy, but also a diluted (scaled) version of the input rate.

Nonetheless, we found the problem of maximization given by (21) for Poisson fading channel to be equivalent to the problem of maximization for Poisson channel defined by Y. Kabanov as [30]

$$\mathcal{C} = \max_{0 < \lambda < \Lambda} \left[\frac{\lambda}{\Lambda} \phi(\Lambda) - \phi(\lambda) \right], \quad (22)$$

where $\lambda \in [0, \Lambda]$ denotes the input rate. By comparing (21) and (22),

$$\mu \equiv \lambda/\Lambda \quad \text{and} \quad s\Lambda \equiv \Lambda. \quad (23)$$

Hence, as long as the receiver has the CSI as advocated in [35], the scaling of the output rate *does not* impose principal changes to the method of maximization described by Kabanov.

Following this important inference and Section III, we define the *upper bound on the capacity for the bipartite synaptic Poisson channel with constant vesicle release probability* as given by (24), where $\mu_{max}^{(b)}$ is obtained by maximizing (21) with $s = p_{rel}$, i.e.,

$$\mu_{max}^{(b)} = \frac{\lambda_0}{p_{rel}\Lambda} \left[\frac{1}{e} \left(1 + \frac{p_{rel}\Lambda}{\lambda_0}\right)^{(1+(p_{rel}\Lambda)^{-1}\lambda_0)} - 1 \right]. \quad (25)$$

C. Noisy and Unreliable Vesicle Release with Time-Varying Release Probability

If the probabilities from the previous scenario are time-varying, i.e., S in (20) is a random variable, and the receiver possesses perfect CSI while the transmitter has no CSI, the corresponding optical channel capacity is found similarly (refer to (21)). The maximum of the averaged conditional mutual information is then given as [35]

$$\mathcal{C} = \max_{0 \leq \mu \leq \sigma} \mathbb{E}[\mu\phi(S\Lambda) - \phi(\mu S\Lambda)], \quad (26)$$

where the expectation is taken over the distribution of random variable S , and μ is the probability of the channel input taking the value Λ , σ is the ratio of average-to-peak power, $0 \leq \sigma \leq 1$, and S is the channel fade.

Considering the vesicle release probability P_{rel} in synaptic communication system is time-varying, as defined by (4), the *upper bound on the capacity for the bipartite synaptic Poisson channel with time-varying vesicle release probability* is

$$\mathcal{C}_{UB}^{(c)} = \max_{0 \leq \mu \leq \sigma} \mathbb{E}[\mu\phi(P_{rel}\Lambda) - \phi(\mu P_{rel}\Lambda)], \quad (27)$$

where the expectation is taken over the distribution of the random variable P_{rel} .

D. Noisy and Unreliable Bipartite Synapse

The most complex and realistic scenario has the added effects of unreliability incurred by the neurotransmitter propagation through the synaptic cleft and the ligand-binding

mechanism. The output rate of the Poisson channel is then directed by the intensity

$$\lambda_2(t) = P_s(t)P_b(t) [\lambda_0 + P_{rel}(t)\lambda_1(t)]. \quad (28)$$

The effect of spontaneous vesicle release $P_s(t)P_b(t)\lambda_0$ and the probability product $P_{rel}(t)P_s(t)P_b(t)$ in (28) now correspond to the “dark current” λ_0 and the channel fade $S(t)$ in (20), respectively. Nevertheless, the problem of calculating the channel capacity for a noisy and unreliable bipartite synapse is *not* equivalent to the problem of calculating the capacity for the optical Poisson fading channel, where the output rate is given by (20).

Namely, the assumption in Section IV-B is that the noise (λ_0) and signal sources ($\lambda'_1 = P_{rel}(t)\lambda_1$) are independent and thus uncorrelated (refer to (19)). If $X = \lambda_0$ and $Y = \lambda'_1$, then $\text{Cov}[X, Y] = 0$, i.e., $\mathbb{E}[XY] = \mathbb{E}[X]\mathbb{E}[Y]$. In the current scenario where the system model is described with (28), the multiplicative term $P_s(t)P_b(t)$ is associated with the intensity of both the noise and the signal sources. As described in Section II, the neurotransmitter propagation probability P_s follows a Bernoulli distribution, i.e., $P_s = p_s$ for a given synapse, and is connected to the diffusion and neurotransmitters being lost in the cleft. This is independent on both signal and noise, regardless the quantity of the particles. The neurotransmitter binding probability P_b is though random and time varying, and is connected to the ligand-binding mechanism. Now, if $X = \lambda_0$, $Y = \lambda'_1$ and $Z = p_s P_b$, we consider the uncorrelatedness of the variables $U = XZ = p_s P_b \lambda_0$ and $V = YZ = p_s P_b \lambda'_1$ (see (28)). We assume the variables X, Y, Z are pairwise uncorrelated ($\text{Cov}[X, Y] = 0$, $\text{Cov}[X, Z] = 0$ and $\text{Cov}[Y, Z] = 0$), although not pairwise independent as P_b depends on the neurotransmitter concentration at the post-synaptic side as given by (9), where the neurotransmitter concentration is dependent on the input signal λ_1 . Under these assumptions⁵

$$\text{Cov}[U, V] = \text{Cov}[XZ, YZ] = \mathbb{E}[X]\mathbb{E}[Y]\text{Var}[Z] \geq 0.$$

Hence, the right hand side is zero when $\text{Var}[Z] = 0$, i.e., the ligand-binding mechanism is either ideal or the neurotransmitter binding probability follows a Bernoulli distribution, i.e., $P_b = p_b$ for a given synapse⁶. Only then the variables $U = XZ$ and $V = YZ$ are uncorrelated and the problem of calculating the channel capacity for a noisy and unreliable bipartite synapse is equivalent to the problem of calculating the capacity for the optical Poisson fading channel, where the output rate is given by (20). Otherwise, the computation of the capacity remains an issue.

With the simplified amendment that both the neurotransmitter propagation and binding follow a Bernoulli distribution, the *upper bound on the capacity for the bipartite synaptic Poisson channel with constant vesicle release probability*, $\mathcal{C}_{UB}^{(d)}$, follows similarly from (24). The *upper bound on the*

⁵We use result of $\text{Cov}[AB, CD]$, where A, B, C and D are jointly distributed random variables, and the conventional asymptotic approximation procedure from [40, page 232]. Given $A = X, B = Z, C = Y$ and $D = Z$ that are pairwise uncorrelated we yield the result presented.

⁶We are not interested in scenarios when $\mathbb{E}[X] = \mathbb{E}[\lambda_0] = 0$ and/or $\mathbb{E}[Y] = \mathbb{E}[P_{rel}\lambda_1] = 0$.

capacity for the bipartite synaptic Poisson channel with time-varying vesicle release probability, $\mathcal{C}_{UB}^{(d')}$, follows similarly from (27).

E. Noisy and Unreliable Tripartite Synapse

In the set-up with the astocytic feedback to the pre-synaptic terminal, the spontaneous vesicle release is time-varying, $\lambda_0(t)$, as mentioned earlier. To compute the capacity for the tripartite synapse, we adapt the result provided by Frey [32] who considered the information capacity of the Poisson channel with random noise intensity in optical channels.

Hence, the *upper bound on the capacity for the tripartite synaptic Poisson channel with constant vesicle release probability* is given as

$$\mathcal{C}_{UB}^{(e')} = \frac{1}{T} \int_0^T \mathcal{C}_{UB}^{(d')}(\lambda, \Lambda, \mu) dt. \quad (29)$$

The *upper bound on the capacity for the tripartite synaptic Poisson channel with time-varying vesicle release probability* is given as

$$\mathcal{C}_{UB}^{(e'')} = \frac{1}{T} \int_0^T \mathcal{C}_{UB}^{(d'')}(\lambda, \Lambda, \mu) dt. \quad (30)$$

The capacities $\mathcal{C}_{UB}^{(d')}$ and $\mathcal{C}_{UB}^{(d'')}$ are defined in previous subsection for the case when both the neurotransmitter propagation and binding follow a Bernoulli distribution. The results from (29) and (30) are proved by the proof of Theorem 1 given in [32] by making changes analogous to those made by Davis in Kabanov’s proof [31].

V. ANALYTICAL EXAMPLES

The best way to test the credibility of theoretical models would be to estimate the rates from experimental data and then compare results. To this end, we must collect data to estimate experimental information limits, which is a challenging task as we discussed in the Introduction. Instead, we provide a graphical evaluation of the closed-form expressions for the information capacity bounds derived in Sections IV-A, IV-B and IV-C. The provided numbers depend on selection of parameters (λ_0 and p_{rel}) that are cell-type specific.

The upper bound on information rate from (18) for bipartite synaptic Poisson channel with reliable vesicle release considered in Section IV-A is plotted in Fig. 3 given various rates λ_0 . As observed, the information capacity is higher for less noisy synapses. Given $\lambda_0 = 0.1$ [s⁻¹], the information rate goes up to 36.5 [bit/s] and saturates for peak spiking rates higher than 37 [spike/s]. For lower peak spiking rates, the information rate rises exponentially. Conversely, for very noisy synapses, the maximum information capacity is lower, e.g., given $\lambda_0 = 20$ [s⁻¹], the capacity reduces to 20 [bit/s], but becomes less sensitive as λ_0 increases.

The upper bound on the information rate for an unreliable (constant p_{rel}) and noisy bipartite synapse considered in Section IV-B is plotted in Fig. 4 given various rates λ_0 and vesicle release probability $p_{rel} = 0.4$, and in Fig. 5 given various probabilities p_{rel} and rate $\lambda_0 = 10$ [s⁻¹]. Relative to Fig. 3, the information rates in Fig. 4 are lower. From

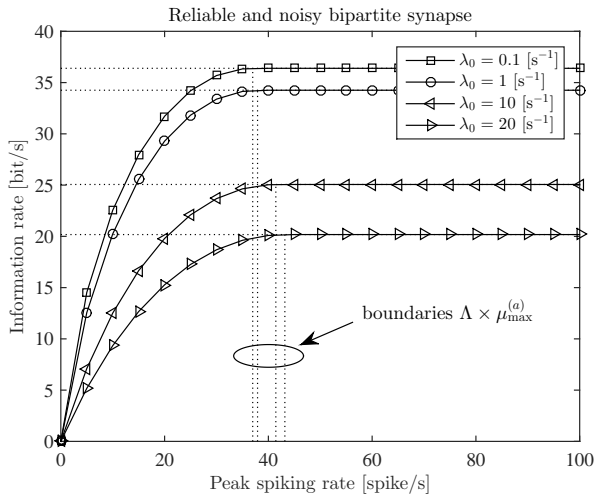


Fig. 3. The upper bound on information rate as a function of the peak spiking rate Λ given various rates λ_0 for a synapse with reliable vesicle release, $p_{rel} = 1$. Vertical line segments show boundaries $\Lambda \times \mu_{max}^{(a)}$.

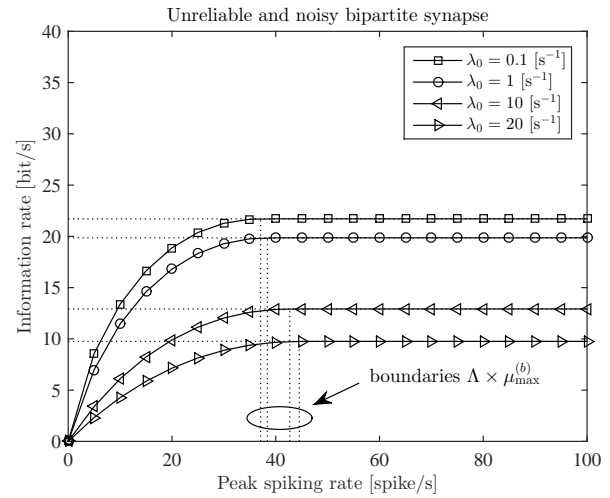


Fig. 4. The upper bound on information rate as a function of the peak spiking rate Λ given various rates λ_0 for an unreliable synapse, $p_{rel} = 0.4$. Vertical line segments show boundaries $\Lambda \times \mu_{max}^{(b)}$.

Fig. 4, given $\lambda_0 = 0.1 [s^{-1}]$, the information rate goes up to 22 [bit/s] and saturates for peak spiking rates higher than 37 [spike/s]. For lower peak spiking rates, the information rate rises exponentially. As in Fig. 3, for very noisy synapses, the maximum information capacity is lower, e.g., given $\lambda_0 = 20 [s^{-1}]$, the capacity drops below 10 [bit/s], but becomes less sensitive as λ_0 increases. Ultimately, as shown in Fig. 5, intuitively higher information rates are observed for higher p_{rel} values. With $p_{rel} = 1$, the information capacity coincides with the capacity in (18).

The upper bound on the information rate for an unreliable and noisy bipartite synapse considered in Section IV-C is plotted in Fig. 6 by assuming the probability of the vesicle release P_{rel} follows a beta distribution with shaping parameters $\alpha = 2, \beta = 5$ (shown in the inset). We select beta density function after considering Fig. 2b from [41]. This result is essential for evaluation of the capacity upper bounds for unreliable synapses with time-varying vesicle release. Given $\lambda_0 = 1 [s^{-1}]$, the information rate goes up to 9 [bit/s] and saturates for peak spiking rates higher than 40 [spike/s].

Albeit Manwani and Koch derived theoretical lower bounds on the information capacity of a simple model of the bipartite synapse [21], it is not instructive to compare the results as the underlying system models are different.

VI. SIMULATION EXAMPLE

In this example, we simulate a hippocampal synapse to record the signals transmitted, as well as other ionic and numerical quantities, from which we can learn about the synaptic behavior and extract parameters requisite for capacity computation. The primary aim is to identify real set-up with some of the analysis in Section IV, and then practically gain insight into the theoretical information capacity bounds. To this end, we develop the simulator based on the validated models from computational neuroscience:

- 1) Pinsky-Rinzel model [19], [25] - The model is a 2-compartment reduction of the complex 19-compartment

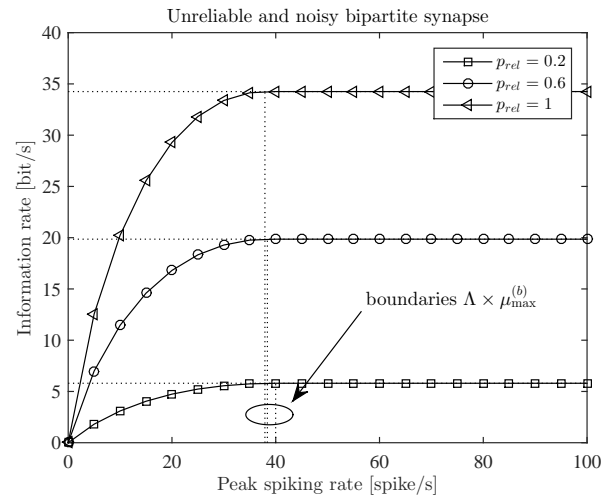


Fig. 5. The upper bound on information rate as a function of the peak spiking rate Λ given various probabilities p_{rel} and $\lambda_0 = 10 [s^{-1}]$ for an unreliable synapse. Vertical line segments show boundaries $\Lambda \times \mu_{max}^{(b)}$.

cable model by Traub [42]. The model is shown to be able to describe experimental observations on neuronal behaviour, and is used in our study for current and potential dynamics of the pre-synaptic hippocampal neuron;

- 2) Li-Rinzel model [19], [20], [26] - The model is able to describe experimental observations on synaptic behaviour when the astrocyte is connected to the synapse, and is used to quantify the feedback from the astrocyte to the pre-synaptic terminal;
- 3) Bertram-Sherman-Stanley model [27] - The model is used to describe the process of neurotransmitter release that is based on the finding that release can be gated during the opening of individual Ca^{2+} channels. In this four-gate model, all gates must be activated for release to occur;
- 4) Wang-Buzsaki model [43] - The model is used for current and potential dynamics of the post-synaptic neuron.

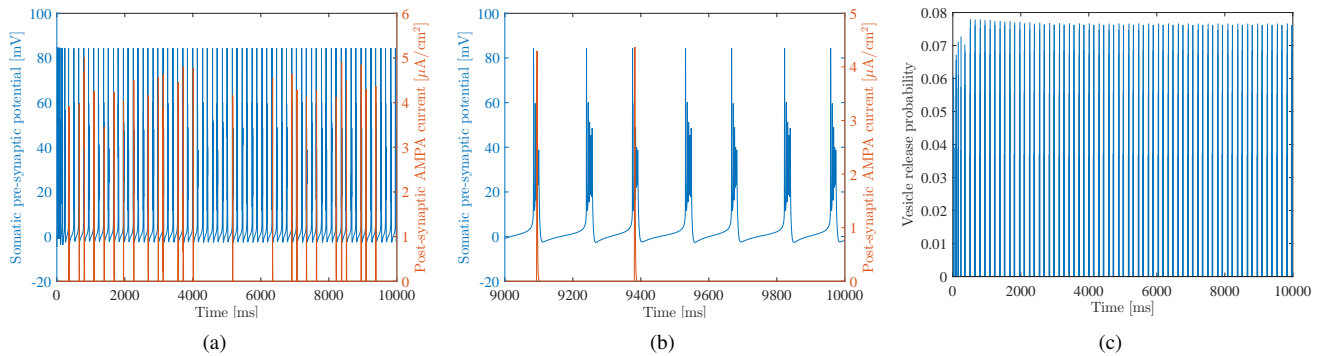


Fig. 7. Simulation time $T_s = 10$ [s]; (a) A realization of the spiking sequence (blue) with rate $\lambda_1 = 35.2$ [spike/s] (spiking threshold is set to 30 mV) at the pre-synaptic neuron given the amplitude of stimulus somatic current $I_s = 1.5$ [$\mu\text{A}/\text{cm}^2$]; Corresponding current response (orange) at the post-synaptic neuron. (b) A realization of the spiking sequence and post-synaptic current response in $t \in [9000, 10000]$ ms; this plot visualizes the regular patterns of spiking bursts that are not visible in (a). (c) Vesicle release probability at the pre-synaptic neuron.

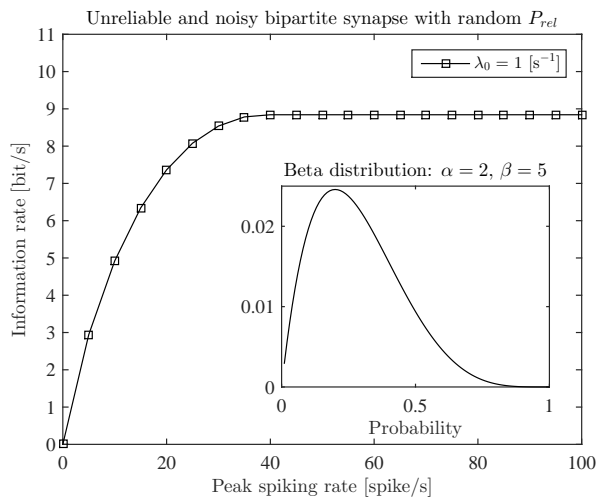


Fig. 6. The upper bound on information rate as a function of the peak spiking rate Λ given beta distributed P_{rel} and $\lambda_0 = 1$ [s^{-1}] for an unreliable synapse.

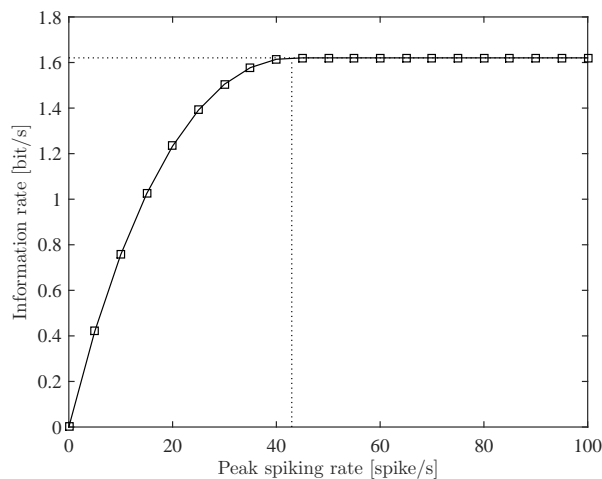


Fig. 8. The upper bound on the capacity for the realistic bipartite synapse with $P_{rel} \approx 0.078$ and $\lambda_0 = 1.44$ s^{-1} .

The simulation framework is implemented in Julia [44] – an open-source high-level dynamic programming language that

provides high performance of utilized computational models of neurons.

Referring back to Section IV that provides expressions to calculate the upper bounds on the information capacity under different set-ups, one needs to estimate the effect of spontaneous vesicle release, λ_0 , and probabilities P_{rel} , P_s and P_b . With a simulator based on the models provided above, we are though not able to extract the neurotransmitter propagation and neurotransmitter binding probabilities required in Sections IV-D and IV-E. This limitation can potentially be overcome with additional computational models that unlike the ones used in the simulation framework treat the diffusive propagation of particles and the ligand-binding mechanism. Instead, we will try to identify simulated scenarios with their simplifications where P_s and P_b are not involved.

A. Realistic Bipartite Synapse

For the bipartite synapse, the intracellular calcium concentration can be approximated as constant at the time instants of action potential arrivals (the envelope of the concentration is constant), as demonstrated later in Fig. 9(b). Thus, $\lambda_0(t) = \lambda_0$, and is estimated from (11), where $a_1 = 7181$ μM , $a_2 = 606$ μM , and $a_3 = 100$ ms^{-1} [20].

To determine the vesicle release probability, P_{rel} , a detailed inspection is required. In general, the vesicle release probability is calculated from (4) as a time-varying temporal function. Nonetheless, this may not strictly apply to all bipartite set-ups. Namely, Fig. 7 illustrates the scenario when the bipartite synapse is stimulated with the somatic current $I_s = 1.5$ [$\mu\text{A}/\text{cm}^2$], leading to approximately constant vesicle release probability observed after arrivals of action potentials (see Fig. 7(c)). In realistic scenarios, the vesicle release probability has a small value – in the simulated scenario, $P_{rel} \approx 0.078$.

Albeit not plotted in Fig. 7, the intracellular calcium concentration is approximately constant after arrivals of action potentials, and $[\text{Ca}^{2+}]_{pre} = [\text{Ca}^{2+}]_{AP} = 427$ μM , which lead to $\lambda_0 = 1.44$ s^{-1} . With requisite parameters estimated, the upper bound on the capacity for the simulated bipartite synapse is computed with (24), and plotted in Fig. 8 as a function of the peak spiking rate. Thereby, the simulated bipartite synapse limits the information rate to 1.6 [bit/s].

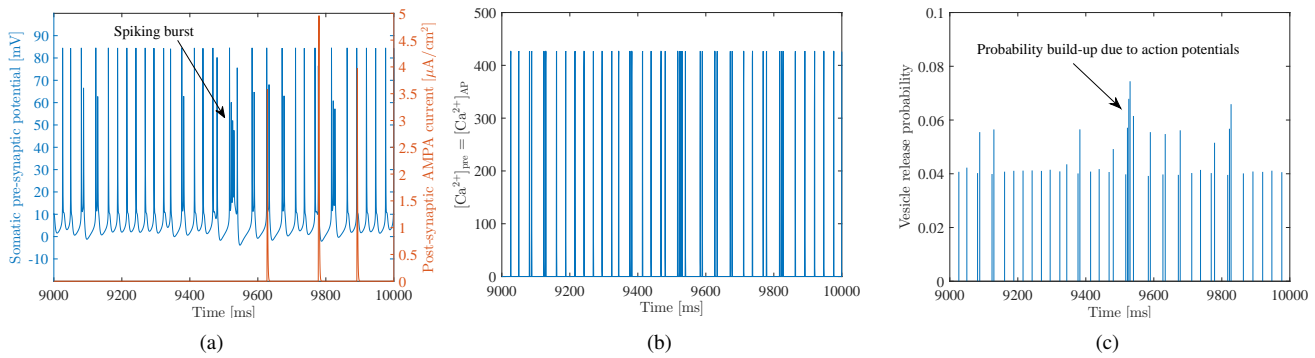


Fig. 9. Amplitude of stimulus somatic current $I_s = 2 [\mu\text{A}/\text{cm}^2]$; simulation time $T_s = 10 [\text{s}]$; time window presented $T_w = 1 [\text{s}]$. (a) A realization of the spiking sequence (blue) with rate $\lambda_1 = 46.6 [\text{spike}/\text{s}]$ at the pre-synaptic neuron; Corresponding current response (orange) at the post-synaptic neuron. (b) The intracellular calcium concentration at the pre-synaptic terminal. (c) Vesicle release probability at the pre-synaptic neuron with notable modulation from the spiking bursts.

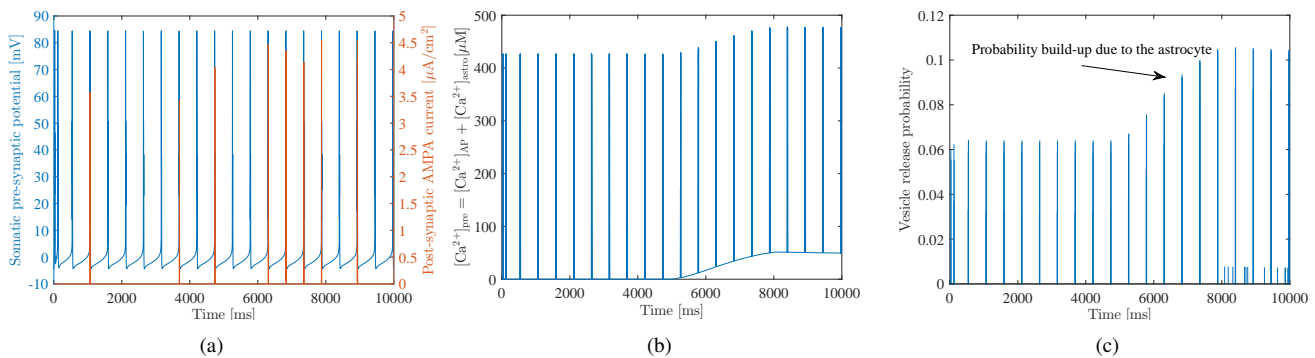


Fig. 10. Amplitude of stimulus somatic current $I_s = 0.7 [\mu\text{A}/\text{cm}^2]$; simulation time $T_s = 10 [\text{s}]$. (a) A realization of the spiking sequence (blue) with rate $\lambda_1 = 4 [\text{spike}/\text{s}]$ at the pre-synaptic neuron; Corresponding current response (orange) at the post-synaptic neuron. (b) The intracellular calcium concentration at the pre-synaptic terminal with notable modulation from the astrocytic activity. (c) Vesicle release probability at the pre-synaptic neuron with notable modulation from the astrocytic activity.

In addition, we infer that an arbitrary realistic bipartite set-up can also be approximated with scenario considered in Section IV-B where (24) is used to define the upper bound on the information capacity when the stimulus is within a certain range – for hippocampal neurons we determine empirically that the somatic current is within the range $[0, 1.5] [\mu\text{A}/\text{cm}^2]$.

On the other hand, when the stimulus is strong ($I_s > 1.5 [\mu\text{A}/\text{cm}^2]$), as in the scenario presented in Fig. 9, the vesicle release probability is not constant after arrivals of spikes due to the spiking bursts that appear. Thereby, an arbitrary realistic bipartite set-up corresponds to the scenario considered in Section IV-C where (27) is used to define the upper bound on the information capacity when the stimulus is strong ($I_s > 1.5 [\mu\text{A}/\text{cm}^2]$). Note that (27) requires the probability distribution of P_{rel} .

B. Realistic Tripartite Synapse

For the tripartite synapse, the envelope of the intracellular calcium concentration is time-varying due to the astrocytic contribution. This is shown in Fig. 10 where the tripartite synapse is stimulated with the somatic current $I_s = 0.7 [\mu\text{A}/\text{cm}^2]$, leading also to the time-varying vesicle release probability observed after arrivals of action potentials (see Fig. 10(c)). The upper bound on the information capacity

for the tripartite synapse is thus computed from simplified versions of (29) and (30) (the effects of P_s and P_b are neglected) regardless the intensity of the stimulus.

Note, however, that the feedback from astrocytic activity to the intracellular calcium concentration can be insignificant in some intervals disguising the change in the vesicle release probability P_{rel} . As many things around neurons, the modulation of the probability P_{rel} due to the astrocyte is stochastic in nature.

VII. CONCLUSION AND FUTURE WORK

The neuronal nano-network is developed by the evolution's guidelines and is the most fascinating, complex, and advanced intra-body nano-network that effectively coordinates and influences the activity of all voluntary and involuntary operations in the body. The way information theory characterizes the neuronal channels and their ability to convey neurotransmitters that encode the information, despite the disturbances introduced, is very interesting to neuroscience and ICT community that develops neural-like nano-networks. Unlike previous contributions, in this study we have provided the capacity upper bounds of synaptic transmission between two neurons.

Specifically, we have first identified the synaptic transmission channel with optical communication channel, indicating all the relevant analogies. Then, we have considered different set-ups with progressive complexity, that are, however, found in the brain, to provide the capacity upper bounds of noisy bipartite and tripartite synapses. The effects of uncertainties confined to the neurotransmitter release, transmission, and binding have been modeled. Analytical evaluations of the closed-form expressions for the information capacity bounds have been derived for the noisy bipartite synapse with reliable vesicle release, and noisy bipartite synapse with unreliable vesicle release with constant and time-varying release probabilities. The results show that a few tenths of bits per second can possibly be achieved, depending on the noise and reliability levels in the synapse. Conversely, if the probabilities associated with unreliability along the remaining communication pathway between neurons undergo distribution other than Bernoulli's, the closed-form formulas for the upper bound on the information channel capacity remain unknown.

Moreover, realistic synapses have been simulated using a developed simulator to record quantities that are indicating synaptic nature and are required for the information capacity evaluation. The simulated hippocampal bipartite synapse is shown to convey up to 1.6 [bit/s]. Also, for the simulated tripartite synapse we extracted the quantities that suggest the way the information capacity should be computed.

Eventually, to find more exact capacity bounds for neuronal synapses, it is of primary importance to determine closed-form bounds without CSI in general future research efforts. As a future work, we aim at discovering the information flow achievable by the whole neuron. To this end, we must consider the capacity of several synapses constituted by two observed neurons (and the astrocyte) that lead to spiking at the post-synaptic neuron. The evaluation of the multiple-synapse capacity requests a new system model with encompassed role of the multiple-access interference that has not been considered in this paper. Moreover, we indicate a verification of theoretical results derived in this study using experimental simulations and real data.

ACKNOWLEDGEMENT

The authors would like to thank Kimmo Kansanen for constructive discussions, and the referees for their excellent and constructive feedback.

REFERENCES

- [1] L. Galluccio, S. Palazzo, and G. E. Santagati, "Modeling signal propagation in nanomachine-to-neuron communications," *Nano Communication Networks*, vol. 2, no. 4, pp. 213–222, 2011.
- [2] E. Balevi and O. Akan, "A physical channel model for nanoscale neuro-spike communications," *IEEE Transactions on Communications*, vol. 61, no. 3, pp. 1178–1187, 2013.
- [3] D. Malak and O. Akan, "A communication theoretical analysis of synaptic multiple-access channel in hippocampal-cortical neurons," *IEEE Transactions on Communications*, vol. 61, no. 6, pp. 2457–2467, June 2013.
- [4] D. Song, R. Chan, V. Marmarelis, R. Hampson, S. Deadwyler, and T. Berger, "Nonlinear dynamic modeling of spike train transformations for hippocampal-cortical prostheses," *IEEE Transactions on Biomedical Engineering*, vol. 54, no. 6, pp. 1053–1066, 2007.

- [5] J. Suzuki, S. Balasubramaniam, S. Pautot, V. Perez Meza, and Y. Koucheryavy, "A service-oriented architecture for body area nanonetworks with neuron-based molecular communication," *Mobile Networks and Applications*, vol. 19, no. 6, pp. 707–717, 2014.
- [6] C. Koch, *Biophysics of computation: Information processing in single neurons*. New York: Oxford University Press, 1999.
- [7] K. G. Oweiss, *Statistical Signal Processing for Neuroscience and Neurotechnology*, K. G. Oweiss, Ed. Elsevier, 2010.
- [8] T. M. Cover and J. A. Thomas, *Elements of Information Theory*. New York: Wiley, 2006.
- [9] R. B. Stein, "The information capacity of nerve cells using a frequency code," *Biophysical Journal*, vol. 6, no. 7, pp. 797–826, 1967.
- [10] A. Borst and F. E. Theunissen, "Information theory and neural coding," *Nature Neuroscience*, vol. 2, no. 11, pp. 947–957, 1999.
- [11] S. Ikeda and J. Manton, "Spiking neuron channel," in *IEEE International Symposium on Information Theory, ISIT 2009*, June 2009, pp. 1589–1593.
- [12] P. Suksompong and T. Berger, "Capacity analysis for integrate-and-fire neurons with descending action potential thresholds," *IEEE Transactions on Information Theory*, vol. 56, no. 2, pp. 838–851, Feb 2010.
- [13] T. Berger and W. Levy, "A mathematical theory of energy efficient neural computation and communication," *IEEE Transactions on Information Theory*, vol. 56, no. 2, pp. 852–874, Feb 2010.
- [14] M. Veletic, P. Floor, Z. Babic, and I. Balasingham, "Peer-to-peer communication in neuronal nano-network," *IEEE Transactions on Communications*, vol. PP, no. 99, pp. 1–1, 2016.
- [15] Y. Yu, M. Crumiller, B. Knight, and E. Kaplan, "Estimating the amount of information carried by a neuronal population," *Frontiers in Computational Neuroscience*, vol. 4, pp. 1–10, 2010.
- [16] P. Dayan and L. F. Abbott, *Theoretical Neuroscience: Computational and Mathematical Modeling of Neural Systems*. The MIT Press, Cambridge, Massachusetts, London, England, 2001.
- [17] F. Mesiti, M. Veletic, P. A. Floor, and I. Balasingham, "Astrocyte-neuron communication as cascade of equivalent circuits," *Nano Communication Networks*, vol. 6, no. 4, pp. 183 – 197, 2015, bio-Nano Communications Networks and Systems.
- [18] S. Nadkarni and P. Jung, "Dressed neurons: modeling neural-glia interactions," *Physical Biology*, vol. 1, no. 1, p. 35, 2004.
- [19] —, "Modeling synaptic transmission of the tripartite synapse," *Physical Biology*, vol. 4, no. 1, p. 1, 2007. [Online]. Available: <http://stacks.iop.org/1478-3975/4/i=1/a=001>
- [20] S. Nadkarni, P. Jung, and H. Levine, "Astrocytes optimize the synaptic transmission of information," *PLoS Computational Biology*, vol. 4, p. e1000088, May 2008.
- [21] A. Manwani and C. Koch, "Detecting and estimating signals over noisy and unreliable synapses: information-theoretic analysis," *Neural computation*, vol. 13, no. 1, pp. 1–33, Jan. 2001.
- [22] A. Cacciapuoti, M. Caleffi, and A. Piras, "Modeling the dynamic processing of the presynaptic terminals for intra-body nanonetworks," *IEEE Transactions on Communications*, vol. PP, no. 99, pp. 1–1, 2016.
- [23] M. J. Berry and M. Meister, "Refractoriness and neural precision," *The Journal of Neuroscience*, vol. 18, no. 6, pp. 2200–2211, 1998.
- [24] M. Veletic, F. Mesiti, P. A. Floor, and I. Balasingham, "Communication theory aspects of synaptic transmission," in *IEEE International Conference on Communications (IEEE ICC 2015)*, June 2015, pp. 2719–2724.
- [25] P. F. Pinsky and J. Rinzel, "Intrinsic and network rhythmogenesis in a reduced Traub model for ca3 neurons," *Journal of Computational Neuroscience*, no. 1, pp. 39–40, 1994.
- [26] Y. X. Li and J. Rinzel, "Equations for InsP3 receptor-mediated [ca2+]i oscillations derived from a detailed kinetic model: A Hodgkin-Huxley like formalism," *Journal of Theoretical Biology*, vol. 166, no. 4, pp. 461 – 473, 1994.
- [27] R. Bertram, A. Sherman, and E. F. Stanley, "Single-domain/bound calcium hypothesis of transmitter release and facilitation," *Journal of Neurophysiology*, vol. 75, no. 5, pp. 1919–1931, 1996.
- [28] Y. Chahibi and I. Akyildiz, "Molecular communication noise and capacity analysis for particulate drug delivery systems," *IEEE Transactions on Communications*, vol. 62, no. 11, pp. 3891–3903, Nov 2014.
- [29] M. Pierobon and I. Akyildiz, "Noise analysis in ligand-binding reception for molecular communication in nanonetworks," *IEEE Transactions on Signal Processing*, vol. 59, no. 9, pp. 4168–4182, Sept 2011.
- [30] Y. M. Kabanov, "The capacity of a channel of the Poisson type," *Theory of Probability & Its Applications*, vol. 23, no. 1, pp. 143–147, 1978.
- [31] M. Davis, "Capacity and cutoff rate for Poisson-type channels," *IEEE Transactions on Information Theory*, vol. 26, no. 6, pp. 710–715, Nov 1980.

- [32] M. R. Frey, "Information capacity of the Poisson channel," *IEEE Transactions on Information Theory*, vol. 37, no. 2, pp. 244–256, March 1991.
- [33] S. Shamai and A. Lapidoth, "Bounds on the capacity of a spectrally constrained poisson channel," *IEEE Transactions on Information Theory*, vol. 39, no. 1, pp. 19–29, Jan 1993.
- [34] S. Hranilovic and F. R. Kschischang, "Capacity bounds for power- and band-limited optical intensity channels corrupted by gaussian noise," *IEEE Transactions on Information Theory*, vol. 50, no. 5, pp. 784–795, May 2004.
- [35] K. Chakraborty and P. Narayan, "The Poisson fading channel," *IEEE Transactions on Information Theory*, vol. 53, no. 7, pp. 2349–2364, July 2007.
- [36] I. Bar-David, "Communication under the Poisson regime," *IEEE Transactions on Information Theory*, vol. 15, no. 1, pp. 31–37, Jan 1969.
- [37] S. Verdú, "Poisson communication theory," in *The International Technon Communication Day in honor of Israel Bar-David*, March 1999, invited talk.
- [38] "Electrophysiological values of maximum firing rate across neuron types from literature," http://neuroelectro.org/ephys_prop/35/, accessed: 15/07/2016.
- [39] S. B. Laughlin, "Energy as a constraint on the coding and processing of sensory information," *Current Opinion in Neurobiology*, vol. 11, no. 4, pp. 475 – 480, 2001.
- [40] M. G. Kendall and A. Stuart, *The Advanced Theory of Statistics, Vol. 1*. London: Griffin, 1963.
- [41] T. Branco and K. Staras, "The probability of neurotransmitter release: variability and feedback control at single synapses," *Nature Reviews Neuroscience*, vol. 10, no. 5, pp. 373–383, 2009.
- [42] R. Traub, R. Wong, R. Miles, and H. Michelson, "A model of a ca3 hippocampal pyramidal neuron incorporating voltage-clamp data on intrinsic conductances," *Journal of Neurophysiology*, vol. 2, no. 66, 1991.
- [43] X. J. Wang and G. Buzsaki, "Gamma oscillation by synaptic inhibition in a hippocampal interneuronal network model," *The Journal of Neuroscience*, no. 16, pp. 6402 – 6413, 1996.
- [44] P. NumFocus. (2016) Julia: an open-source programing language. [Online]. Available: <http://www.julialang.org/>



Pål Anders Floor received the B.Sc. degree from Gjøvik University College (HIG), Gjøvik, Norway, in 2001, the M.Sc. degree in 2003, and the Ph.D. degree in 2008, both from the Department of Electronics and Telecommunications, Norwegian University of Science and Technology (NTNU), Trondheim, Norway. All three degrees are in electrical engineering.

He was working as a Post. Doc. at the Intervention Center at Oslo University Hospital as well as the Institute of Clinical Medicine at the University of Oslo from 2008-2013. He is currently a Post. Doc. at the Department of Electronics and Telecommunications at NTNU. His research interests include joint source-channel coding, information theory and signal processing applied on point-to-point links, in small and large networks, as well as in Neuroscience, and lightweight cryptography.



Youssef Chahibi (S'13) received the Ph.D. and the M.S. degree from the Georgia Institute of Technology, Atlanta, USA, in 2012 and 2016, respectively, and the Diplôme d'Ingénieur in Telecommunications and Networks from Institut National Polytechnique de Toulouse, France, in 2011.

He was a physical-layer Engineer at Alcatel-Lucent, Antwerp, Belgium, during 2011. He joined the BWN lab of the School of Electrical and Computer Engineering, Georgia Institute of Technology, Atlanta, in January 2012 and graduated with a Ph.D. in August 2016 under the supervision of Prof. Ian F. Akyildiz. In Summer 2014, he was a guest research scholar at the Nano Communication Center (NCC) at Tampere University of Technology collaborating with Dr. Balasubramaniam and Prof. Koucheryavy, and during 2015, he was a fellow of the Research Council of Norway at the Norwegian University of Science and Technology (NTNU) in Trondheim, Norway, collaborating with Prof. Balasingham's Biomedical Sensor Network Research Group. His research interests include nanoscale biologically-inspired communications, nanonetworks and drug delivery systems.



Ilango Balasingham received the M.Sc. and Ph.D. degrees from the Department of Electronics and Telecommunications, Norwegian University of Science and Technology (NTNU), Trondheim, Norway in 1993 and 1998, respectively, both in signal processing. He performed his Master's degree thesis at the Department of Electrical and Computer Engineering, University of California Santa Barbara, USA.

From 1998 to 2002, he worked as a Research Scientist developing image and video streaming solutions for mobile handheld devices at Fast Search & Transfer ASA, Oslo, Norway, which is now part of Microsoft Inc. Since 2002 he has been with the Intervention Center, Oslo University Hospital, Oslo, Norway as a Senior Research Scientist, where he heads the Wireless Sensor Network Research Group. He was appointed as a Professor in Signal Processing in Medical Applications at NTNU in 2006. His research interests include super robust short range communications for both in-body and on-body sensors, body area sensor network, microwave short range sensing of vital signs, short range localization and tracking mobile sensors, and nano-neural communication networks. He has authored or co-authored 192 journal and conference papers, 5 book chapters, 42 abstracts, 2 patents, and 10 articles in media. Ilango has given 14 invited/keynotes at the international conferences.

In addition to organizing special sessions and workshops on wireless medical technology at the major conferences and symposiums, he served as General Chair of the 2012 Body Area Networks (BODYNETS) conference and serves as TPC Co-Chair of the 2015 ACM NANOCOM and Area Editor of Elsevier Nano Communication Networks. He is a Senior IEEE member.



Mladen Veletić received the B.Sc. and M.Sc. degrees in electronics and telecommunications from the Faculty of Electrical Engineering, University of Banja Luka (UNIBL), Banja Luka, Bosnia & Herzegovina in 2010 and 2012, respectively.

Since January 2013, he is a Ph.D student at the Department of Electronics and Telecommunications, Norwegian University of Science and Technology (NTNU), Trondheim, Norway, and the Faculty of Electrical Engineering, UNIBL, as a scholar within HERD/ICT NORBAS project under reference 2011/1383 supported by the Norwegian Ministry of Foreign Affairs. His research interests include wireless communications, positioning in cellular networks, molecular and nano-neural communications.

Mladen Veletić is a Student IEEE member. He was awarded a Gold Plaque from the UNIBL for his achievements throughout the undergraduate education.